arXiv:1211.6214v1 [nucl-th] 27 Nov 2012

Interplay between Spin Polarization and Color Superconductivity in High Density Quark Matter

Yasuhiko TSUE,[1,2] João da PROVIDÊNCIA,[3] Constança PROVIDÊNCIA,[3]
Masatoshi YAMAMURA[4] and Henrik BOHR[5]

[1] *Centro de Física Computacional, Departamento de Física, Universidade de Coimbra, 3004-516 Coimbra, Portugal*
[2] *Physics Division, Faculty of Science, Kochi University, Kochi 780-8520, Japan*
[3] *Departamento de Física, Universidade de Coimbra, 3004-516 Coimbra, Portugal*
[4] *Department of Pure and Applied Physics, Faculty of Engineering Science, Kansai University, Suita 564-8680, Japan*
[5] *Department of Physics, B.307, Danish Technical University, DK-2800 Lyngby, Denmark*

It is indicated that there is a possibility of spin polarization in the quark matter at high density due to the tensor-type four-point interaction between quarks. The realized phase is determined by the comparison of pressure of quark spin polarized phase with that of the two-flavor color superconducting phase which may appear in high density quark matter. It is shown that the quark spin polarized phase is realized at rather high density, while the two-flavor color superconducting phase is realized at a lower density region.

§1. Introduction

Under extreme conditions such as high temperature and/or high baryon density, it is interesting to study the behavior of the quark and gluonic matter and/or hadronic matter governed by quantum chromodynamics (QCD) in the context of the physics of the relativistic heavy ion collisions and of the interior of compact stars. At low temperature and high density region[1)] such as the interior of a neutron star, it is widely investigated and pointed out that various phases may be realized, for example, various meson condensed phases in hadronic matter,[2)] the two-flavor color superconducting (2SC) and the color-flavor locked (CFL) phases,[3)–5)] the quarkyonic phase[6)] and the quark ferromagnetic phase[7)] in quark matter, and so forth. Especially, we may conjecture that the quark ferromagnetic phase exists at high density quark matter, since the existence of magnetar was reported.[8)] In a preceding work,[7)] the pseudovector-type interaction between quarks was considered and it was pointed out that the quark spin polarization was realized. However, it was shown that, the quark spin alignment disappears, if the quark mass is zero, for example, in the chiral symmetric phase.[9)]

Recently, the present authors have indicated that the quark spin polarization occurs at high density quark matter even in the chiral symmetric phase due to the tensor-type four-point interaction between quarks, which leads to the quark ferromagnetization.[10),11)] In that paper, it has been shown that a second-order phase transition occurs from normal quark phase to quark spin polarized phase. However, in quark matter at high baryon density, it is believed that the two-flavor color superconducting phase appears. Thus, it is interesting to investigate the stability of the quark spin polarized phase against the 2SC phase.

In this paper, we investigate the color-symmetric superconducting phase[12)] and the quark spin polarized phase and clarify which phase is stable by using the Nambu-Jona-Lasinio (NJL) model[13)] including quark-pair interaction[14)] and the tensor-type four-point interaction.[10),11)] The quark-pair interaction is derived by the Fierz transformation from the original NJL model Lagrangian. We consider the quark-pairing gap $\mathit{\Delta}$ and the quark spin polarization F separately such that $\mathit{\Delta} \neq 0$ or $F \neq 0$ leads to the 2SC phase or quark spin polarized phase, respectively. In this paper, the system is treated by the mean field approximation and the BCS state is introduced.[15)]

This paper is organized as follows: In the next section, the basic Hamiltonian is introduced and expressions of the Hamiltonian under some basis sets are given. In Appendix A, one of the expressions of Hamiltonian is given in which the good helicity states are used. In §3, the BCS state is defined and the thermodynamic potential is derived. In §4, numerical results and discussions are given and the last section is devoted to a summary and concluding remarks.

§2. NJL model with tensor interaction

2.1. *Basic Hamiltonian*

Let us start with the following Lagrangian density:

$$\begin{aligned}
&\mathcal{L} = \mathcal{L}_0 + \mathcal{L}_S + \mathcal{L}_T + \mathcal{L}_c \ , \\
&\mathcal{L}_0 = \bar{\psi} i\gamma^\mu \partial_\mu \psi \ , \\
&\mathcal{L}_S = G_S((\bar{\psi}\psi)^2 + (\bar{\psi} i\gamma_5 \vec{\tau}\psi)^2) \ , \\
&\mathcal{L}_T = -\frac{G}{4}\left((\bar{\psi}\gamma^\mu\gamma^\nu\vec{\tau}\psi)(\bar{\psi}\gamma_\mu\gamma_\nu\vec{\tau}\psi) + (\bar{\psi}i\gamma_5\gamma^\mu\gamma^\nu\psi)(\bar{\psi}i\gamma_5\gamma_\mu\gamma_\nu\psi)\right) \ , \\
&\mathcal{L}_c = \frac{G_c}{2}\sum_{A=2,5,7}\left((\bar{\psi}i\gamma_5\tau_2\lambda_A\psi^C)(\bar{\psi}^C i\gamma_5\tau_2\lambda_A\psi) + (\bar{\psi}\tau_2\lambda_A\psi^C)(\bar{\psi}^C\tau_2\lambda_A\psi)\right) \ . \qquad (2\cdot 1)
\end{aligned}$$

Here, $\psi^C = C\bar{\psi}^T$ with $C = i\gamma^2\gamma^0$ being the charge conjugation operator. Also, τ_2 is the second component of the Pauli matrices representing the isospin $su(2)$-generator and λ_A are the antisymmetric Gell-Mann matrices representing the color $su(3)_c$-generator. As is well known, the Lagrangian density $\mathcal{L}_0 + \mathcal{L}_S$ corresponds to the original NJL model. We add $\mathcal{L}_c$ which can be derived by the Fierz transformation from $\mathcal{L}_S$ and represents the quark-pair interaction. Also, we introduce $\mathcal{L}_T$ which represents the tensor-type interaction between quarks.

In this paper, we concentrate on quark matter at high baryon density where the chiral symmetry is restored in the density region considered here. Thus, the chiral condensate, $\langle\bar{\psi}\psi\rangle$, is assumed to be equal to zero in this high density region. Under the mean field approximation, the above Lagrangian density is recast into

$$\begin{aligned}
&\mathcal{L}^{MF} = \mathcal{L}_0 + \mathcal{L}_T^{MF} + \mathcal{L}_c^{MF} \ , \\
&\mathcal{L}_T^{MF} = -F(\bar{\psi}\mathit{\Sigma}_3\tau_3\psi) - \frac{F^2}{2G} \ ,
\end{aligned}$$

$$
\begin{aligned}
&F = -G\langle\bar{\psi}\Sigma_3\tau_3\psi\rangle \ , \qquad \Sigma_3 = -i\gamma^1\gamma^2 = \begin{pmatrix} \sigma_3 & 0 \\ 0 & \sigma_3 \end{pmatrix} \ , \\
&\mathcal{L}_c^{MF} = -\frac{1}{2}\sum_{A=2,5,7}(\Delta\bar{\psi}^C i\gamma_5\tau_2\lambda_A + h.c.) - \frac{3\Delta^2}{2G_c} \ , \\
&\Delta_A = \Delta_A^* = -G_c\langle\bar{\psi}i\gamma_5\tau_2\lambda_A\psi\rangle \ , \qquad \Delta = \Delta_2 = \Delta_5 = \Delta_7 \ ,
\end{aligned} \tag{2·2}
$$

where *h.c.* represents the Hermitian conjugate term of the preceding one. Here, we used Dirac representation for the Dirac gamma matrices and σ_3 represents the third component of the 2×2 Pauli spin matrices. The symbol $\langle\cdots\rangle$ represents the expectation value with respect to a vacuum state. The expectation value F corresponds to the order parameter of the spin alignment which leads to quark ferromagnetization. The expectation value Δ corresponds to the quark-pair condensate which means the existence of the color superconducting phase if $\Delta \neq 0$. Here, in order to insure color symmetry we assume that all quark-pair condensates have the same expectation values, $\Delta_2 = \Delta_5 = \Delta_7$.

The mean field Hamiltonian density with quark chemical potential μ is easily obtained as

$$
\begin{aligned}
&\mathcal{H}_{MF} - \mu\mathcal{N} = \mathcal{K}_0 + \mathcal{H}_T^{MF} + \mathcal{H}_c^{MF} \ , \\
&\quad \mathcal{K}_0 = \bar{\psi}(-\boldsymbol{\gamma}\cdot\boldsymbol{\nabla} - \mu\gamma_0)\psi \ , \\
&\quad \mathcal{H}_T^{MF} = -\mathcal{L}_T^{MF} \ , \qquad \mathcal{H}_c^{MF} = -\mathcal{L}_c^{MF}
\end{aligned} \tag{2·3}
$$

with $\mathcal{N} = \psi^\dagger\psi$. In the basis of good helicity states, the relevant combination of the mean field Hamiltonian $H_{MF} = \int d^3\boldsymbol{x}\mathcal{H}_{MF}$ and the quark number $N = \int d^3\boldsymbol{x}\mathcal{N}$ is given by

$$
\begin{aligned}
H_{MF} - \mu N = &\sum_{\boldsymbol{p}\eta\tau\alpha}\left[(p-\mu)c^\dagger_{\boldsymbol{p}\eta\tau\alpha}c_{\boldsymbol{p}\eta\tau\alpha} - (p+\mu)\tilde{c}^\dagger_{\boldsymbol{p}\eta\tau\alpha}\tilde{c}_{\boldsymbol{p}\eta\tau\alpha}\right] \\
&+F\sum_{\boldsymbol{p}\eta\tau\alpha}\phi_\tau\left[\frac{\sqrt{p_1^2+p_2^2}}{p}\left(c^\dagger_{\boldsymbol{p}\eta\tau\alpha}c_{\boldsymbol{p}-\eta\tau\alpha} + \tilde{c}^\dagger_{\boldsymbol{p}\eta\tau\alpha}\tilde{c}_{\boldsymbol{p}-\eta\tau\alpha}\right)\right. \\
&\qquad\qquad\left. -\eta\frac{p_3}{p}\left(c^\dagger_{\boldsymbol{p}\eta\tau\alpha}\tilde{c}_{\boldsymbol{p}\eta\tau\alpha} + \tilde{c}^\dagger_{\boldsymbol{p}\eta\tau\alpha}c_{\boldsymbol{p}\eta\tau\alpha}\right)\right] \\
&+\frac{\Delta}{2}\sum_{\boldsymbol{p}\eta\alpha\alpha'\alpha''\tau\tau'}(c^\dagger_{\boldsymbol{p}\eta\tau\alpha}c^\dagger_{-\boldsymbol{p}\eta\tau'\alpha'} + \tilde{c}^\dagger_{\boldsymbol{p}\eta\tau\alpha}\tilde{c}^\dagger_{-\boldsymbol{p}\eta\tau'\alpha'} \\
&\qquad\qquad +c_{-\boldsymbol{p}\eta\tau'\alpha'}c_{\boldsymbol{p}\eta\tau\alpha} + \tilde{c}_{-\boldsymbol{p}\eta\tau'\alpha'}\tilde{c}_{\boldsymbol{p}\eta\tau\alpha})\phi_\tau\epsilon_{\alpha\alpha'\alpha''}\epsilon_{\tau\tau'} \\
&+V\cdot\frac{F^2}{2G} + V\cdot\frac{3\Delta^2}{2G_c} \ ,
\end{aligned} \tag{2·4}
$$

where V represents the volume in the box normalization.[*)] Here, $c^\dagger_{\boldsymbol{p}\eta\tau\alpha}$ and $\tilde{c}^\dagger_{\boldsymbol{p}\eta\tau\alpha}$ represent the quark and antiquark creation operators with momentum $\boldsymbol{p}$, helicity

---

[*)] We hope that no confusion may occur although notations V_{cs} and $V(\boldsymbol{p})$ appear later which represent the quark-pair interaction in (2·5) and a matrix in (2·9) diagonalizing a certain part of the Hamiltonian matrix, respectively.

$\eta = \pm$, isospin index $\tau = \pm$ and color α. Further, $\phi_\tau = 1$ for $\tau = 1$ (up quark) and $\phi_\tau = -1$ for $\tau = -1$ (down quark). Also, $\epsilon_{\tau\tau'}$ and $\epsilon_{\alpha\alpha'\alpha''}$ represent the complete antisymmetric tensor for the isospin and color indices. We define $p = \sqrt{p_1^2 + p_2^2 + p_3^2}$ that is the magnitude of momentum.

For later convenience, we rewrite the above Hamiltonian as

$$
\begin{aligned}
&H_{MF} - \mu N = H_{MF}^{SP} - \mu N + V_{cs} + V \cdot \frac{F^2}{2G} + V \cdot \frac{3\mathit{\Delta}^2}{2G_c} \ , \\
&H_{MF}^{SP} - \mu N = \sum_{\boldsymbol{p}\tau\tau'\alpha\alpha'\alpha''} \begin{pmatrix} c^\dagger_{\boldsymbol{p}+\tau\alpha} \\ c^\dagger_{\boldsymbol{p}-\tau\alpha} \\ \tilde{c}^\dagger_{\boldsymbol{p}+\tau\alpha} \\ \tilde{c}^\dagger_{\boldsymbol{p}-\tau\alpha} \end{pmatrix}^T (\kappa - \mu \cdot 1)\delta_{\tau\tau'}\delta_{\alpha\alpha'} \begin{pmatrix} c_{\boldsymbol{p}+\tau'\alpha'} \\ c_{\boldsymbol{p}-\tau'\alpha'} \\ \tilde{c}_{\boldsymbol{p}+\tau'\alpha'} \\ \tilde{c}_{\boldsymbol{p}-\tau'\alpha'} \end{pmatrix} \ , \\
&\kappa = \begin{pmatrix} p & 0 & 0 & 0 \\ 0 & p & 0 & 0 \\ 0 & 0 & -p & 0 \\ 0 & 0 & 0 & -p \end{pmatrix} + \frac{F\tau_3}{p} \begin{pmatrix} 0 & \sqrt{p_1^2+p_2^2} & -p_3 & 0 \\ \sqrt{p_1^2+p_2^2} & 0 & 0 & p_3 \\ -p_3 & 0 & 0 & \sqrt{p_1^2+p_2^2} \\ 0 & p_3 & \sqrt{p_1^2+p_2^2} & 0 \end{pmatrix} \ , \\
&V_{cs} = \frac{\mathit{\Delta}}{2} \sum_{\boldsymbol{p}\eta\alpha\alpha'\alpha''\tau\tau'} (c^\dagger_{\boldsymbol{p}\eta\tau\alpha} c^\dagger_{-\boldsymbol{p}\eta\tau'\alpha'} + \tilde{c}^\dagger_{\boldsymbol{p}\eta\tau\alpha} \tilde{c}^\dagger_{-\boldsymbol{p}\eta\tau'\alpha'} + c_{-\boldsymbol{p}\eta\tau'\alpha'} c_{\boldsymbol{p}\eta\tau\alpha} + \tilde{c}_{-\boldsymbol{p}\eta\tau'\alpha'} \tilde{c}_{\boldsymbol{p}\eta\tau\alpha}) \\
&\qquad\qquad \times \phi_\tau \epsilon_{\alpha\alpha'\alpha''} \epsilon_{\tau\tau'} \ .
\end{aligned}
\tag{2·5}
$$

As for V_{cs}, we can easily sum up with respect to τ and τ' which leads to

$$
V_{cs} = \mathit{\Delta} \sum_{\boldsymbol{p}\eta\alpha\alpha'\alpha''} \epsilon_{\alpha\alpha'\alpha''} (c^\dagger_{\boldsymbol{p}\eta+\alpha} c^\dagger_{-\boldsymbol{p}\eta-\alpha'} + \tilde{c}^\dagger_{\boldsymbol{p}\eta+\alpha} \tilde{c}^\dagger_{-\boldsymbol{p}\eta-\alpha'} + c_{-\boldsymbol{p}\eta-\alpha'} c_{\boldsymbol{p}\eta+\alpha} + \tilde{c}_{-\boldsymbol{p}\eta-\alpha'} \tilde{c}_{\boldsymbol{p}\eta+\alpha}) \ .
\tag{2·6}
$$

2.2. *Expressions of the Hamiltonian under other basis sets*

If the quark-pair condensate $\mathit{\Delta}$ is equal to zero, the operator given by equation (2·5) becomes $H_{MF}^{SP} - \mu N + VF^2/(2G)$. Since the quark number N is already diagonal, let us diagonalize the Hamiltonian matrix κ first. First, we set up $\tau_3 = 1$ because the contribution of $\tau_3 = -1$ is the same as the contribution of $\tau_3 = 1$ as was seen in (2·6), which results in a factor 2. Then, the Hamiltonian matrix κ can be simply expressed as

$$
\kappa = \begin{pmatrix} q & e & -g & 0 \\ e & q & 0 & g \\ -g & 0 & -q & e \\ 0 & g & e & -q \end{pmatrix} \ ,
\tag{2·7}
$$

where $q = p$, $e = F\sqrt{p_1^2 + p_2^2}/p$ and $g = Fp_3/p$. The eigenvalues of κ are easily obtained as

$$
\pm\varepsilon_{\boldsymbol{p}}^{(\pm)} = \pm\sqrt{g^2 + (e \pm q)^2} = \pm\sqrt{p_3^2 + \left(F \pm \sqrt{p_1^2 + p_2^2}\right)^2} \ .
\tag{2·8}
$$

The following matrix is introduced in order to diagonalize the above Hamiltonian matrix:

$$V(\boldsymbol{p})=\begin{pmatrix} \frac{\sqrt{\varepsilon_{\boldsymbol{p}}^{(+)}+e+q}}{2\sqrt{\varepsilon_{\boldsymbol{p}}^{(+)}}} & -\frac{\sqrt{\varepsilon_{\boldsymbol{p}}^{(-)}-e+q}}{2\sqrt{\varepsilon_{\boldsymbol{p}}^{(-)}}} & -\frac{\sqrt{\varepsilon_{\boldsymbol{p}}^{(+)}-e-q}}{2\sqrt{\varepsilon_{\boldsymbol{p}}^{(+)}}} & \frac{\sqrt{\varepsilon_{\boldsymbol{p}}^{(-)}+e-q}}{2\sqrt{\varepsilon_{\boldsymbol{p}}^{(-)}}} \\ \frac{\sqrt{\varepsilon_{\boldsymbol{p}}^{(+)}+e+q}}{2\sqrt{\varepsilon_{\boldsymbol{p}}^{(+)}}} & \frac{\sqrt{\varepsilon_{\boldsymbol{p}}^{(-)}-e+q}}{2\sqrt{\varepsilon_{\boldsymbol{p}}^{(-)}}} & -\frac{\sqrt{\varepsilon_{\boldsymbol{p}}^{(+)}-e-q}}{2\sqrt{\varepsilon_{\boldsymbol{p}}^{(+)}}} & -\frac{\sqrt{\varepsilon_{\boldsymbol{p}}^{(-)}+e-q}}{2\sqrt{\varepsilon_{\boldsymbol{p}}^{(-)}}} \\ -\frac{g}{2\sqrt{\varepsilon_{\boldsymbol{p}}^{(+)}(\varepsilon_{\boldsymbol{p}}^{(+)}+e+q)}} & \frac{g}{2\sqrt{\varepsilon_{\boldsymbol{p}}^{(-)}(\varepsilon_{\boldsymbol{p}}^{(-)}-e+q)}} & -\frac{g}{2\sqrt{\varepsilon_{\boldsymbol{p}}^{(+)}(\varepsilon_{\boldsymbol{p}}^{(+)}-e-q)}} & \frac{g}{2\sqrt{\varepsilon_{\boldsymbol{p}}^{(-)}(\varepsilon_{\boldsymbol{p}}^{(-)}+e-q)}} \\ \frac{g}{2\sqrt{\varepsilon_{\boldsymbol{p}}^{(+)}(\varepsilon_{\boldsymbol{p}}^{(+)}+e+q)}} & \frac{g}{2\sqrt{\varepsilon_{\boldsymbol{p}}^{(-)}(\varepsilon_{\boldsymbol{p}}^{(-)}-e+q)}} & \frac{g}{2\sqrt{\varepsilon_{\boldsymbol{p}}^{(+)}(\varepsilon_{\boldsymbol{p}}^{(+)}-e-q)}} & \frac{g}{2\sqrt{\varepsilon_{\boldsymbol{p}}^{(-)}(\varepsilon_{\boldsymbol{p}}^{(-)}+e-q)}} \end{pmatrix} . \tag{2·9}$$

Then, we can diagonalize the Hamiltonian matrix κ as $V^\dagger \kappa V$. Namely,

$$H_{MF}^{SP}=\sum_{\boldsymbol{p}\tau\alpha}\begin{pmatrix} b_{\boldsymbol{p}+\tau\alpha}^\dagger \\ b_{\boldsymbol{p}-\tau\alpha}^\dagger \\ \tilde{b}_{\boldsymbol{p}+\tau\alpha}^\dagger \\ \tilde{b}_{\boldsymbol{p}-\tau\alpha}^\dagger \end{pmatrix}^T \text{diag } \kappa \begin{pmatrix} b_{\boldsymbol{p}+\tau\alpha} \\ b_{\boldsymbol{p}-\tau\alpha} \\ \tilde{b}_{\boldsymbol{p}+\tau\alpha} \\ \tilde{b}_{\boldsymbol{p}-\tau\alpha} \end{pmatrix} , \tag{2·10}$$

where we define

$$\text{diag } \kappa = \begin{pmatrix} \varepsilon_{\boldsymbol{p}}^{(+)} & 0 & 0 & 0 \\ 0 & \varepsilon_{\boldsymbol{p}}^{(-)} & 0 & 0 \\ 0 & 0 & -\varepsilon_{\boldsymbol{p}}^{(+)} & 0 \\ 0 & 0 & 0 & -\varepsilon_{\boldsymbol{p}}^{(-)} \end{pmatrix} ,$$
$$\begin{pmatrix} b_{\boldsymbol{p}+\tau\alpha} \\ b_{\boldsymbol{p}-\tau\alpha} \\ \tilde{b}_{\boldsymbol{p}+\tau\alpha} \\ \tilde{b}_{\boldsymbol{p}-\tau\alpha} \end{pmatrix} = V^\dagger(\boldsymbol{p}) \begin{pmatrix} c_{\boldsymbol{p}+\tau\alpha} \\ c_{\boldsymbol{p}-\tau\alpha} \\ \tilde{c}_{\boldsymbol{p}+\tau\alpha} \\ \tilde{c}_{\boldsymbol{p}-\tau\alpha} \end{pmatrix} . \tag{2·11}$$

Secondly, let us consider the total Hamiltonian matrix with quark-pair interaction term in the above derived basis. In this basis, V_{cs} in (2·6) is written as

$$V_{cs}=\varDelta \sum_{\boldsymbol{p}\alpha\alpha'\alpha''}\begin{pmatrix} b_{\boldsymbol{p}++\alpha}^\dagger \\ b_{\boldsymbol{p}-+\alpha}^\dagger \\ \tilde{b}_{\boldsymbol{p}++\alpha}^\dagger \\ \tilde{b}_{\boldsymbol{p}-+\alpha}^\dagger \end{pmatrix}^T V^\dagger(\boldsymbol{p})V(-\boldsymbol{p}) \begin{pmatrix} b_{-\boldsymbol{p}+-\alpha'}^\dagger \\ b_{-\boldsymbol{p}--\alpha'}^\dagger \\ \tilde{b}_{-\boldsymbol{p}+-\alpha'}^\dagger \\ \tilde{b}_{-\boldsymbol{p}--\alpha'}^\dagger \end{pmatrix} \epsilon_{\alpha\alpha'\alpha''} . \tag{2·12}$$

Here, if we replace $\boldsymbol{p}$ into $-\boldsymbol{p}$, then q, e, g and $\varepsilon_{\boldsymbol{p}}^{(\pm)}$ in (2·7) are changed or unchanged to q, e, $-g$ and $\varepsilon_{\boldsymbol{p}}^{(\pm)}$. Thus, we obtain

$$V^\dagger(\boldsymbol{p})V(-\boldsymbol{p}) = \begin{pmatrix} \frac{q+e}{\varepsilon_{\boldsymbol{p}}^{(+)}} & 0 & -\frac{|g|}{\varepsilon_{\boldsymbol{p}}^{(+)}} & 0 \\ 0 & \frac{q-e}{\varepsilon_{\boldsymbol{p}}^{(-)}} & 0 & -\frac{|g|}{\varepsilon_{\boldsymbol{p}}^{(-)}} \\ -\frac{|g|}{\varepsilon_{\boldsymbol{p}}^{(+)}} & 0 & -\frac{q+e}{\varepsilon_{\boldsymbol{p}}^{(+)}} & 0 \\ 0 & -\frac{|g|}{\varepsilon_{\boldsymbol{p}}^{(-)}} & 0 & -\frac{q-e}{\varepsilon_{\boldsymbol{p}}^{(-)}} \end{pmatrix} . \qquad (2{\cdot}13)$$

Finally, let us diagonalize the above matrix $V^\dagger(\boldsymbol{p})V(-\boldsymbol{p})$. We introduce the following matrix:

$$W = \begin{pmatrix} -\sqrt{\frac{\varepsilon_{\boldsymbol{p}}^{(+)}+e+q}{2\varepsilon_{\boldsymbol{p}}^{(+)}}} & 0 & \sqrt{\frac{\varepsilon_{\boldsymbol{p}}^{(+)}-e-q}{2\varepsilon_{\boldsymbol{p}}^{(+)}}} & 0 \\ 0 & -\sqrt{\frac{\varepsilon_{\boldsymbol{p}}^{(-)}-e+q}{2\varepsilon_{\boldsymbol{p}}^{(-)}}} & 0 & \sqrt{\frac{\varepsilon_{\boldsymbol{p}}^{(-)}+e-q}{2\varepsilon_{\boldsymbol{p}}^{(-)}}} \\ \frac{|g|}{\sqrt{2\varepsilon_{\boldsymbol{p}}^{(+)}(\varepsilon_{\boldsymbol{p}}^{(+)}+e+q)}} & 0 & \frac{|g|}{\sqrt{2\varepsilon_{\boldsymbol{p}}^{(+)}(\varepsilon_{\boldsymbol{p}}^{(+)}-e-q)}} & 0 \\ 0 & \frac{|g|}{\sqrt{2\varepsilon_{\boldsymbol{p}}^{(-)}(\varepsilon_{\boldsymbol{p}}^{(-)}-e+q)}} & 0 & \frac{|g|}{\sqrt{2\varepsilon_{\boldsymbol{p}}^{(-)}(\varepsilon_{\boldsymbol{p}}^{(-)}+e-q)}} \end{pmatrix} . \qquad (2{\cdot}14)$$

Then, by using the matrix W, the matrix $V^\dagger(\boldsymbol{p})V(-\boldsymbol{p})$ which appears in the quark-pair interaction part can be diagonalized as

$$W^\dagger V^\dagger(\boldsymbol{p})V(-\boldsymbol{p})W = \begin{pmatrix} 1 & 0 & 0 & 0 \\ 0 & 1 & 0 & 0 \\ 0 & 0 & -1 & 0 \\ 0 & 0 & 0 & -1 \end{pmatrix} . \qquad (2{\cdot}15)$$

By introducing new fermion operators $(a_{\boldsymbol{p}\eta\tau\alpha}, a_{\boldsymbol{p}\eta\tau\alpha}^\dagger, \tilde{a}_{\boldsymbol{p}\eta\tau\alpha}, \tilde{a}_{\boldsymbol{p}\eta\tau\alpha}^\dagger)$ by

$$\begin{pmatrix} a_{\boldsymbol{p}+\tau\alpha} \\ a_{\boldsymbol{p}-\tau\alpha} \\ \tilde{a}_{\boldsymbol{p}+\tau\alpha} \\ \tilde{a}_{\boldsymbol{p}-\tau\alpha} \end{pmatrix} = W^\dagger \begin{pmatrix} b_{\boldsymbol{p}+\tau\alpha} \\ b_{\boldsymbol{p}-\tau\alpha} \\ \tilde{b}_{\boldsymbol{p}+\tau\alpha} \\ \tilde{b}_{\boldsymbol{p}-\tau\alpha} \end{pmatrix} , \qquad (2{\cdot}16)$$

the mean field Hamiltonian in which both the quark spin polarization and quark-pair condensate are simultaneously considered can be expressed as

$$\begin{aligned} H_{MF} - \mu N = &\sum_{\boldsymbol{p}\eta\tau\alpha} \left[(\varepsilon_{\boldsymbol{p}}^{(\eta)} - \mu) a_{\boldsymbol{p}\eta\tau\alpha}^\dagger a_{\boldsymbol{p}\eta\tau\alpha} - (\varepsilon_{\boldsymbol{p}}^{(\eta)} + \mu) \tilde{a}_{\boldsymbol{p}\eta\tau\alpha}^\dagger \tilde{a}_{\boldsymbol{p}\eta\tau\alpha} \right] \\ &+ \frac{\Delta}{2} \sum_{\boldsymbol{p}\eta\tau\tau'\alpha\alpha'\alpha''} \left[a_{\boldsymbol{p}\eta\tau\alpha'}^\dagger a_{-\boldsymbol{p}\eta\tau'\alpha''}^\dagger - \tilde{a}_{\boldsymbol{p}\eta\tau\alpha'}^\dagger \tilde{a}_{-\boldsymbol{p}\eta\tau\alpha''}^\dagger + h.c. \right] \epsilon_{\alpha\alpha'\alpha''} \epsilon_{\tau\tau'} \phi_\tau \\ &+ V \cdot \frac{F^2}{2G} + V \cdot \frac{3\Delta^2}{2G_c} . \end{aligned} \qquad (2{\cdot}17)$$

Here, the summation with respect to isospin indices τ and τ' is explicitly rewritten. The above mean field Hamiltonian is the starting point for discussing the quark spin polarized phase and color superconducting phase.

§3. BCS state and thermodynamic potential

We introduce the BCS state following Ref.15):

$$
\begin{aligned}
&|\Psi\rangle = e^{S}|\Psi_0\rangle\ , \qquad |\Psi_0\rangle = \prod_{\boldsymbol{p}\eta\tau\alpha(\varepsilon_{\boldsymbol{p}}^{(\eta)}<\mu)} a_{\boldsymbol{p}\eta\tau\alpha}^{\dagger}|0\rangle\ ,\\
&S = \sum_{\boldsymbol{p}\eta(\varepsilon_{\boldsymbol{p}}^{(\eta)}>\mu)} \frac{K_{\boldsymbol{p}\eta}}{2} \sum_{\alpha\alpha'\alpha''\tau\tau'} a_{\boldsymbol{p}\eta\tau\alpha}^{\dagger} a_{-\boldsymbol{p}\eta\tau'\alpha'}^{\dagger} \epsilon_{\alpha\alpha'\alpha''}\epsilon_{\tau\tau'}\phi_{\tau}\\
&\qquad + \sum_{\boldsymbol{p}\eta(\varepsilon_{\boldsymbol{p}}^{(\eta)}\leq\mu)} \frac{\widetilde{K}_{\boldsymbol{p}\eta}}{2} \sum_{\alpha\alpha'\alpha''\tau\tau'} a_{\boldsymbol{p}\eta\tau\alpha} a_{-\boldsymbol{p}\eta\tau'\alpha'} \epsilon_{\alpha\alpha'\alpha''}\epsilon_{\tau\tau'}\phi_{\tau}\ ,
\end{aligned}
\tag{3·1}
$$

where $|0\rangle$ is the vacuum state with respect to $a_{\boldsymbol{p}\eta\tau\alpha}$ and $K_{\boldsymbol{p}\eta} = K_{-\boldsymbol{p}\eta}$ and $\widetilde{K}_{\boldsymbol{p}\eta} = \widetilde{K}_{-\boldsymbol{p}\eta}$ are satisfied. Here, the contribution of quark-pairing with negative energy is not considered in quark matter. Then, the state $|\Psi\rangle$ is a vacuum state with respect to new operators $d_{\boldsymbol{p}\eta\tau\alpha}$:

$$
d_{\boldsymbol{p}\eta\tau\alpha} = \begin{cases} a_{\boldsymbol{p}\eta\tau\alpha} - K_{\boldsymbol{p}\eta}(a_{-\boldsymbol{p}\eta\tau'\beta}^{\dagger} - a_{-\boldsymbol{p}\eta\tau'\gamma}^{\dagger}) & \text{for}\quad \varepsilon_{\boldsymbol{p}}^{(\eta)} > \mu \\ a_{\boldsymbol{p}\eta\tau\alpha}^{\dagger} + \widetilde{K}_{\boldsymbol{p}\eta}(a_{-\boldsymbol{p}\eta\tau'\beta} - a_{-\boldsymbol{p}\eta\tau'\gamma}) & \text{for}\quad \varepsilon_{\boldsymbol{p}}^{(\eta)} \leq \mu \end{cases}\ , \tag{3·2}
$$

where (α, β, γ) is a cyclic permutation for color indices and $\tau' = -\tau$. For the above operators, the state $|\Psi\rangle$ satisfies the following relation:

$$
d_{\boldsymbol{p}\eta\tau\alpha}|\Psi\rangle = 0\ . \tag{3·3}
$$

The state $|\Psi\rangle$ is identical with the BCS state.

The expectation values for the BCS state are summarized as follows:

$$
\begin{aligned}
&X_{\boldsymbol{p}\eta} = \langle\Psi|a_{\boldsymbol{p}\eta\tau\alpha}^{\dagger}a_{\boldsymbol{p}\eta\tau\alpha'}|\Psi\rangle\ , \qquad (\text{for}\quad \alpha\neq\alpha')\\
&N_{\boldsymbol{p}\eta} = \langle\Psi|a_{\boldsymbol{p}\eta\tau\alpha}^{\dagger}a_{\boldsymbol{p}\eta\tau\alpha}|\Psi\rangle\ ,\\
&D_{\boldsymbol{p}\eta} = \langle\Psi|a_{-\boldsymbol{p}\eta-\tau\alpha'}a_{\boldsymbol{p}\eta\tau\alpha}|\Psi\rangle\ , \qquad (\text{for}\quad \alpha\neq\alpha')\\
&P_{\boldsymbol{p}\eta} = \langle\Psi|a_{-\boldsymbol{p}\eta-\tau\alpha}a_{\boldsymbol{p}\eta\tau\alpha}|\Psi\rangle\ ,
\end{aligned}
\tag{3·4}
$$

where we take $\alpha = 1$ and $\alpha' = 2$ for the following calculations because the color symmetry is retained. We can easily calculate the above expectation values by using the relation (3·3) with (3·2).

For $\varepsilon_{\boldsymbol{p}}^{(\eta)} > \mu$, the following relations are obtained:

$$
\begin{aligned}
&X_{\boldsymbol{p}\eta} = -K_{\boldsymbol{p}\eta}^2 + K_{\boldsymbol{p}\eta}^2(N_{\boldsymbol{p}\eta} - X_{\boldsymbol{p}\eta})\ ,\\
&N_{\boldsymbol{p}\eta} = 2K_{\boldsymbol{p}\eta}^2 - 2K_{\boldsymbol{p}\eta}^2(N_{\boldsymbol{p}\eta} - X_{\boldsymbol{p}\eta})\ ,\\
&D_{\boldsymbol{p}\eta} = K_{\boldsymbol{p}\eta} - 3K_{\boldsymbol{p}\eta}^2 D_{\boldsymbol{p}\eta} + K_{\boldsymbol{p}\eta}^2 P_{\boldsymbol{p}\eta}\ ,\\
&P_{\boldsymbol{p}\eta} = -2K_{\boldsymbol{p}\eta}^2 P_{\boldsymbol{p}\eta}\ .
\end{aligned}
\tag{3·5}
$$

In the same way, for $\varepsilon_{\boldsymbol{p}}^{(\eta)} \le \mu$, the following relations are also obtained:

$$\begin{aligned}
&X_{\boldsymbol{p}\eta} = -\widetilde{K}_{\boldsymbol{p}\eta}^2 (X_{\boldsymbol{p}\eta} - N_{\boldsymbol{p}\eta}) \ , \\
&N_{\boldsymbol{p}\eta} = 1 + 2\widetilde{K}_{\boldsymbol{p}\eta}^2 (X_{\boldsymbol{p}\eta} - N_{\boldsymbol{p}\eta}) \ , \\
&D_{\boldsymbol{p}\eta} = \widetilde{K}_{\boldsymbol{p}\eta} - 3\widetilde{K}_{\boldsymbol{p}\eta}^2 D_{\boldsymbol{p}\eta} - \widetilde{K}_{\boldsymbol{p}\eta}^2 P_{\boldsymbol{p}\eta} \ , \\
&P_{\boldsymbol{p}\eta} = 2\widetilde{K}_{\boldsymbol{p}\eta}^2 P_{\boldsymbol{p}\eta} \ .
\end{aligned} \tag{3·6}$$

As a result, the expectation values are calculated as

For $\varepsilon_{\boldsymbol{p}}^{(\eta)} > \mu$

$$X_{\boldsymbol{p}\eta} = -\frac{K_{\boldsymbol{p}\eta}^2}{1+3K_{\boldsymbol{p}\eta}^2} \ , \quad N_{\boldsymbol{p}\eta} = \frac{2K_{\boldsymbol{p}\eta}^2}{1+3K_{\boldsymbol{p}\eta}^2} \ , \quad D_{\boldsymbol{p}\eta} = \frac{K_{\boldsymbol{p}\eta}}{1+3K_{\boldsymbol{p}\eta}^2} \ , \quad P_{\boldsymbol{p}\eta} = 0 \ , \tag{3·7}$$

For $\varepsilon_{\boldsymbol{p}}^{(\eta)} \le \mu$

$$\begin{aligned}
&X_{\boldsymbol{p}\eta} = \frac{\widetilde{K}_{\boldsymbol{p}\eta}^2}{1+3\widetilde{K}_{\boldsymbol{p}\eta}^2} \ , \quad N_{\boldsymbol{p}\eta} = \frac{1+\widetilde{K}_{\boldsymbol{p}\eta}^2}{1+3\widetilde{K}_{\boldsymbol{p}\eta}^2} = 1 - \frac{2\widetilde{K}_{\boldsymbol{p}\eta}^2}{1+3\widetilde{K}_{\boldsymbol{p}\eta}^2} \ , \\
&D_{\boldsymbol{p}\eta} = \frac{\widetilde{K}_{\boldsymbol{p}\eta}}{1+3\widetilde{K}_{\boldsymbol{p}\eta}^2} \ , \quad P_{\boldsymbol{p}\eta} = 0 \ .
\end{aligned} \tag{3·8}$$

Thus, by summing up with respect to color and isospin indices, we obtain the expectation value of the mean field Hamiltonian for the BCS state as

$$\begin{aligned}
\langle \Psi | H_{MF} - \mu N | \Psi \rangle = 3 &\sum_{\boldsymbol{p}\eta\tau(\varepsilon_{\boldsymbol{p}}^{(\eta)} > \mu)} \left[(\varepsilon_{\boldsymbol{p}}^{(\eta)} - \mu) \frac{2K_{\boldsymbol{p}\eta}^2}{1+3K_{\boldsymbol{p}\eta}^2} + 2\Delta \frac{K_{\boldsymbol{p}\eta}}{1+3K_{\boldsymbol{p}\eta}^2} \right] \\
+3 &\sum_{\boldsymbol{p}\eta\tau(\varepsilon_{\boldsymbol{p}}^{(\eta)} \le \mu)} \left[(\varepsilon_{\boldsymbol{p}}^{(\eta)} - \mu) \left(1 - \frac{2\widetilde{K}_{\boldsymbol{p}\eta}^2}{1+3\widetilde{K}_{\boldsymbol{p}\eta}^2} \right) + 2\Delta \frac{\widetilde{K}_{\boldsymbol{p}\eta}}{1+3\widetilde{K}_{\boldsymbol{p}\eta}^2} \right] \\
&+V \cdot \frac{F^2}{2G} + V \cdot \frac{3\Delta^2}{2G_c} \ .
\end{aligned} \tag{3·9}$$

In order to determine the BCS state, namely, to determine the variational variables $K_{\boldsymbol{p}\eta}$ and $\widetilde{K}_{\boldsymbol{p}\eta}$, we introduce new variational variables $\theta_{p\eta}$ and $\tilde{\theta}_{p\eta}$ instead of $K_{\boldsymbol{p}\eta}$ and $\widetilde{K}_{\boldsymbol{p}\eta}$:

$$\begin{aligned}
&\sin\theta_{p\eta} = \frac{\sqrt{3}K_{\boldsymbol{p}\eta}}{\sqrt{1+3K_{\boldsymbol{p}\eta}^2}} \ , \qquad \cos\theta_{p\eta} = \frac{1}{\sqrt{1+3K_{\boldsymbol{p}\eta}^2}} \ , \\
&\sin\tilde{\theta}_{p\eta} = \frac{\sqrt{3}\widetilde{K}_{\boldsymbol{p}\eta}}{\sqrt{1+3\widetilde{K}_{\boldsymbol{p}\eta}^2}} \ , \qquad \cos\tilde{\theta}_{p\eta} = \frac{1}{\sqrt{1+3\widetilde{K}_{\boldsymbol{p}\eta}^2}} \ .
\end{aligned} \tag{3·10}$$

Thus, the Hamiltonian and color superconducting gap Δ can be expressed in terms of $\theta_{p\eta}$ and $\tilde{\theta}_{p\eta}$ as

$$\langle \Psi | H_{MF} - \mu N | \Psi \rangle = 2 \sum_{\boldsymbol{p}\eta(\varepsilon_{\boldsymbol{p}}^{(\eta)} > \mu)} \left[2(\varepsilon_{\boldsymbol{p}}^{(\eta)} - \mu) \sin^2\theta_{p\eta} + 2\sqrt{3}\Delta \sin\theta_{p\eta} \cos\theta_{p\eta} \right]$$

$$
\begin{aligned}
&+2 \sum_{\boldsymbol{p}\eta(\varepsilon_{\boldsymbol{p}}^{(\eta)}\leq\mu)} \left[(\varepsilon_{\boldsymbol{p}}^{(\eta)}-\mu)(3-2\sin^2\tilde{\theta}_{p\eta})+2\sqrt{3}\Delta\sin\tilde{\theta}_{p\eta}\cos\tilde{\theta}_{p\eta}\right] \\
&+V\cdot\frac{F^2}{2G}+V\cdot\frac{3\Delta^2}{2G_c}\ , \qquad (3\cdot 11)
\end{aligned}
$$

$$
\begin{aligned}
\Delta=\Delta_2=\Delta_5=\Delta_7 &= -G_c\cdot\frac{1}{V}\sum_{\boldsymbol{p}\eta\beta\gamma\tau}\langle\Psi|a_{\boldsymbol{p}\eta\tau\beta}^{\dagger}a_{-\boldsymbol{p}\eta-\tau\gamma}^{\dagger}|\Psi\rangle \\
&= -2G_c\left(\frac{1}{V}\sum_{\boldsymbol{p}\eta\tau(\varepsilon_{\boldsymbol{p}}^{(\eta)}>\mu)}\frac{K_{\boldsymbol{p}\eta}}{1+3K_{\boldsymbol{p}\eta}^2}+\frac{1}{V}\sum_{\boldsymbol{p}\eta\tau(\varepsilon_{\boldsymbol{p}}^{(\eta)}\leq\mu)}\frac{\widetilde{K}_{\boldsymbol{p}\eta}}{1+3\widetilde{K}_{\boldsymbol{p}\eta}^2}\right) \\
&= -\frac{4G_c}{\sqrt{3}}\left(\frac{1}{V}\sum_{\boldsymbol{p}\eta(\varepsilon_{\boldsymbol{p}}^{(\eta)}>\mu)}\sin\theta_{p\eta}\cos\theta_{p\eta}+\frac{1}{V}\sum_{\boldsymbol{p}\eta(\varepsilon_{\boldsymbol{p}}^{(\eta)}\leq\mu)}\sin\tilde{\theta}_{p\eta}\cos\tilde{\theta}_{p\eta}\right)\ . \qquad (3\cdot 12)
\end{aligned}
$$

Here, in the first line in (3·11) and the third line in (3·12), the isospin indices are summed up and an extra factor 2 appears with respect to the corresponding expression in 12). Also, in the second line in (3·12), color indices, β and γ, are summed up and an extra factor 2 also appears.

Next, we impose the minimization condition for $\langle\Psi|H_{MF}-\mu N|\Psi\rangle$ with respect to Δ, $\theta_{p\eta}$ and $\tilde{\theta}_{p\eta}$. First, we impose the minimization condition with respect to Δ:

$$
\frac{\partial}{\partial\Delta}\langle\Psi|H_{MF}-\mu N|\Psi\rangle=0\ . \qquad (3\cdot 13)
$$

This minimization condition leads to the gap equation in (3·12) exactly. Secondly, we minimize $\langle\Psi|H_{MF}-\mu N|\Psi\rangle$ with respect to $\theta_{p\eta}$ and $\tilde{\theta}_{p\eta}$:

$$
\frac{\partial}{\partial\theta_{p\eta}}\langle\Psi|H_{MF}-\mu N|\Psi\rangle=0\ , \qquad \frac{\partial}{\partial\tilde{\theta}_{p\eta}}\langle\Psi|H_{MF}-\mu N|\Psi\rangle=0\ , \qquad (3\cdot 14)
$$

which lead to the following equations:

$$
\begin{aligned}
(\varepsilon_{\boldsymbol{p}}^{(\eta)}-\mu)\sin 2\theta_{p\eta}+\sqrt{3}\Delta\cos 2\theta_{p\eta}&=0\ , \\
-(\varepsilon_{\boldsymbol{p}}^{(\eta)}-\mu)\sin 2\tilde{\theta}_{p\eta}+\sqrt{3}\Delta\cos 2\tilde{\theta}_{p\eta}&=0\ .
\end{aligned} \qquad (3\cdot 15)
$$

Thus, we obtain $\tan 2\theta_{p\eta}=-\sqrt{3}\Delta/(\varepsilon_{\boldsymbol{p}}^{(\eta)}-\mu)$ and $\tan 2\tilde{\theta}_{p\eta}=\sqrt{3}\Delta/(\varepsilon_{\boldsymbol{p}}^{(\eta)}-\mu)$ which gives

$$
\begin{aligned}
\sin\theta_{p\eta}^2&=\frac{1}{2}\left[1-\frac{\varepsilon_{\boldsymbol{p}}^{(\eta)}-\mu}{\sqrt{(\varepsilon_{\boldsymbol{p}}^{(\eta)}-\mu)^2+3\Delta^2}}\right]\ , \\
\sin\tilde{\theta}_{p\eta}^2&=\frac{1}{2}\left[1+\frac{\varepsilon_{\boldsymbol{p}}^{(\eta)}-\mu}{\sqrt{(\varepsilon_{\boldsymbol{p}}^{(\eta)}-\mu)^2+3\Delta^2}}\right]\ .
\end{aligned} \qquad (3\cdot 16)
$$

Since the variational parameters $\theta_{p\eta}$ and $\tilde{\theta}_{p\eta}$ are determined completely, namely, $K_{\boldsymbol{p}\eta}$ and $\widetilde{K}_{\boldsymbol{p}\eta}$ are determined, the BCS state is obtained.

Thus, we can derive the thermodynamic potential $\Phi(\Delta, F, \mu)$ at zero temperature from (3·11) with (3·16) as

$$\begin{aligned}\Phi(\Delta, F, \mu) &= \frac{1}{V}\langle\Phi|H_{MF} - \mu N|\Phi\rangle \\ &= 2\cdot\frac{1}{V}\sum_{\boldsymbol{p}\eta(\varepsilon_{\boldsymbol{p}}^{(\eta)}\leq\mu)}\left[2(\varepsilon_{\boldsymbol{p}}^{(\eta)} - \mu) - \sqrt{(\varepsilon_{\boldsymbol{p}}^{(\eta)} - \mu)^2 + 3\Delta^2}\right] \\ &\quad +2\cdot\frac{1}{V}\sum_{\boldsymbol{p}\eta(\varepsilon_{\boldsymbol{p}}^{(\eta)}>\mu)}^{\Lambda}\left[(\varepsilon_{\boldsymbol{p}}^{(\eta)} - \mu) - \sqrt{(\varepsilon_{\boldsymbol{p}}^{(\eta)} - \mu)^2 + 3\Delta^2}\right] \\ &\quad +\frac{F^2}{2G} + \frac{3\Delta^2}{2G_c}\ , \end{aligned} \tag{3·17}$$

where $\varepsilon_{\boldsymbol{p}}^{(\pm)} = \sqrt{p_3^2 + \left(F \pm \sqrt{p_1^2 + p_2^2}\right)^2}$. Here, we explicitly introduce and write a three momentum cutoff parameter Λ. The gap equation in (3·12), that is $\partial\Phi(\Delta, F, \mu)/\partial\Delta = 0$, is obtained as

$$\Delta\left[2\cdot\frac{1}{V}\sum_{\boldsymbol{p}\eta=\pm}^{\Lambda}\frac{1}{\sqrt{(\varepsilon_{\boldsymbol{p}}^{(\eta)} - \mu)^2 + 3\Delta^2}} - \frac{1}{G_c}\right] = 0\ . \tag{3·18}$$

§4. Numerical results and discussions

In this section, we investigate the possible phases with $F = 0$ and $\Delta \neq 0$ or with $F \neq 0$ and $\Delta = 0$ at high density, namely, two-flavor color superconducting phase or spin polarized phase, respectively. First, in the quark spin polarized phase with $\Delta = 0$, the thermodynamic potential reduces to

$$\Phi(\Delta = 0, F, \mu) = 6\cdot\frac{1}{V}\sum_{\boldsymbol{p}\ (\varepsilon_{\boldsymbol{p}}^{(+)}\leq\mu)}(\varepsilon_{\boldsymbol{p}}^{(+)} - \mu) + 6\cdot\frac{1}{V}\sum_{\boldsymbol{p}\ (\varepsilon_{\boldsymbol{p}}^{(-)}\leq\mu)}(\varepsilon_{\boldsymbol{p}}^{(-)} - \mu) + \frac{F^2}{2G}\ , \tag{4·1}$$

where it should be noted that $\sqrt{(\varepsilon_{\boldsymbol{p}}^{(\eta)} - \mu)^2} = \varepsilon_{\boldsymbol{p}}^{(\eta)} - \mu$ for $\varepsilon_{\boldsymbol{p}}^{(\eta)} > \mu$ or $-(\varepsilon_{\boldsymbol{p}}^{(\eta)} - \mu)$ for $\varepsilon_{\boldsymbol{p}}^{(\eta)} < \mu$, respectively, when (4·1) is derived from (3·17). Of course, the sum over momentum is replaced by the momentum-integration as

$$\frac{1}{V}\sum_{\boldsymbol{p}} \longrightarrow \int\frac{d^3\boldsymbol{p}}{(2\pi)^3}\ . \tag{4·2}$$

Then, the thermodynamic potential derived here is identical with one which has been previously obtained by the present authors, that is, Eq.(3.1) in Ref. 10).*) Thus, the thermodynamic potential with $\mathit{\Delta} = 0$ has already been given in 10) in the analytical form as

---

*) In Eq.(3.1) in Ref.10), F-integration has to be carried out.

$$\mathit{\Phi}(\mathit{\Delta} = 0, F, \mu) = \begin{cases} \dfrac{F^2}{2G} - \dfrac{1}{\pi^2}\Bigg[\dfrac{\sqrt{\mu^2 - F^2}}{4}(3F^2\mu + 2\mu^3) \ +F\mu^3 \arctan \dfrac{F}{\sqrt{\mu^2 - F^2}} & \\ \qquad\qquad -\dfrac{F^4}{4} \ln \dfrac{\mu + \sqrt{\mu^2 - F^2}}{F}\Bigg] & \text{for} \quad F < \mu \\ \dfrac{F^2}{2G} - \dfrac{1}{2\pi}\mu^3 F & \text{for} \quad F > \mu \end{cases} . \tag{4·3}$$

If the minimum of thermodynamic potential exists in the range of $F < \mu$, the gap equation for F is derived from $\partial\mathit{\Phi}(\mathit{\Delta} = 0, F, \mu)/\partial F = 0$ which leads to

$$F = \frac{G}{\pi^2}\left[2F\mu\sqrt{\mu^2 - F^2} + \mu^3 \arctan \frac{F}{\sqrt{\mu^2 - F^2}} - F^3 \ln \frac{\mu + \sqrt{\mu^2 - F^2}}{F}\right] . \tag{4·4}$$

In the other case, namely $F = 0$ case, the two-flavor color superconducting phase may be realized with $\mathit{\Delta} \neq 0$. When $F = 0$, the quasiparticle energy $\varepsilon_{\boldsymbol{p}}^{(\eta)} = p$ is obtained for $\eta = \pm$. The thermodynamic potential (3·17) is then evaluated as

$$\begin{aligned} \mathit{\Phi}(\mathit{\Delta}, F = 0, \mu) = 4 \cdot \frac{1}{V}\sum_{p<\mu}\Big(2(p - \mu) - \sqrt{(p - \mu)^2 + 3\mathit{\Delta}^2}\Big) \\ +4 \cdot \frac{1}{V}\sum_{p>\mu}^{\mathit{\Lambda}}\Big((p - \mu) - \sqrt{(p - \mu)^2 + 3\mathit{\Delta}^2}\Big) + \frac{3\mathit{\Delta}^2}{2G_c} . \end{aligned} \tag{4·5}$$

After replacement of the sum over momentum into momentum-integration in (4·2), the analytical form of the thermodynamic potential is obtained with a three-momentum cutoff parameter $\mathit{\Lambda}$:

$$\begin{aligned} \mathit{\Phi}(\mathit{\Delta}, F = 0, \mu) = {} & \frac{3\mathit{\Delta}^2}{2G_c} - \frac{\mu^4}{6\pi^2} + \frac{\mathit{\Lambda}^4}{2\pi^2} - \frac{2\mu\mathit{\Lambda}^3}{3\pi^2} \\ & -\frac{1}{12\pi^2}\Bigg[(2\mu^3 - 39\mathit{\Delta}^2\mu)(\sqrt{\mu^2 + 3\mathit{\Delta}^2} - \sqrt{(\mu - \mathit{\Lambda})^2 + 3\mathit{\Delta}^2}) \\ & \qquad +(6\mathit{\Lambda}^3 + 9\mathit{\Delta}^2\mathit{\Lambda} - 2\mathit{\Lambda}^2\mu - 2\mathit{\Lambda}\mu^2)\sqrt{(\mu - \mathit{\Lambda})^2 + 3\mathit{\Delta}^2} \\ & \qquad +3(12\mathit{\Delta}^2\mu^2 - 9\mathit{\Delta}^4) \ln \frac{\mathit{\Lambda} - \mu + \sqrt{(\mu - \mathit{\Lambda})^2 + 3\mathit{\Delta}^2}}{-\mu + \sqrt{\mu^2 + 3\mathit{\Delta}^2}}\Bigg] . \end{aligned} \tag{4·6}$$

The gap equation becomes

$$\begin{aligned} \frac{1}{\pi^2}\Bigg[& -3\mu\sqrt{\mu^2 + 3\mathit{\Delta}^2} + (3\mu + \mathit{\Lambda})\sqrt{(\mu - \mathit{\Lambda})^2 + 3\mathit{\Delta}^2} \\ & +(2\mu^2 - 3\mathit{\Delta}^2) \ln \frac{\mathit{\Lambda} - \mu + \sqrt{(\mu - \mathit{\Lambda})^2 + 3\mathit{\Delta}^2}}{-\mu + \sqrt{\mu^2 + 3\mathit{\Delta}^2}}\Bigg] = \frac{1}{G_c} . \end{aligned} \tag{4·7}$$

Table I. Parameter set

Λ / GeV	G / GeV^{-2}	G_c / GeV^{-2}
0.631	20.0	6.6

In both the cases, the quark number density ρ is calculated from the thermodynamical relation as

$$\rho = -\frac{\partial \Phi(\Delta, F, \mu)}{\partial \mu} \ . \tag{4·8}$$

In our model Hamiltonian, the model parameters are G, G_c and Λ. In the original NJL model, the coupling strength G_S appears where $G_S = 5.5$ GeV^{-2} is adopted[16) although this parameter does not appear explicitly in the model considered here. Then, following Ref.14), the strength of the quark-pair interaction, G_c, is taken[*) as $(G_c/2)/G_S = 0.6$. Thus, we adopt $G_c = 6.6$ GeV^{-2}. As for the three-momentum cutoff Λ, a standard value[16) is adopted here, namely, $\Lambda = 0.631$ GeV. If the tail stretching beyond the Fermi momentum of occupation number should be fully taken into account in the BCS theory, a larger value of three-momentum cutoff should be adopted such as $\Lambda = 0.8$ GeV.[15) However, it will be later seen that the tail of the occupation number is already sufficiently taken into account in the case $\Lambda = 0.631$ GeV. As for G in the strength of the tensor-type interaction between quarks, we put $G = 20$ GeV^{-2}, which was used in our previous paper.[10) As was discussed in Ref.10), if the effect of the vacuum polarization is taken into account, the coupling constant G should be replaced to the renormalized coupling G_r in which $1/G_r = 1/G - \Lambda^2/\pi^2$. Then, $G_r = 20$ GeV^{-2} corresponds to the bare coupling $G = 11.1$ GeV^{-2} for $\Lambda = 0.631$ GeV or $G = 8.7$ GeV^{-2} for $\Lambda = 0.8$ GeV. Thus, the strengths of the quark-pairing and tensor-type interactions are comparable. The parameter set used here is summarized in Table 1.

The thermodynamic potential is numerically estimated in two phases, namely, color superconducting phase with $F = 0$ and $\Delta \neq 0$ and quark spin polarized phase with $F \neq 0$ and $\Delta = 0$, separately. We compare the pressure in the color superconducting phase with that in the quark spin polarized phase. The pressure p is given by

$$p = -\Phi(\Delta, F, \mu) \ . \tag{4·9}$$

In Fig.1 (a), the pressures for normal (thin curve), two-flavor color superconducting (dash-dotted curve) and quark spin polarized (solid curve) phases are shown in the case of $\Lambda = 0.631$ GeV as functions with respect to quark chemical potential μ. Up to $\mu = 0.442$ GeV, the two-flavor color superconducting (2SC) phase is realized. However, above $\mu = 0.442$ GeV, the quark spin polarized phase is realized. In Fig. 1 (b), details are depicted around $\mu \approx 0.442$ GeV. The value of chemical potential in the phase transition point is 0.442 GeV, which leads to the 2SC phase up to $\mu = 0.442$ GeV. Thus, it is enough to include the effects of the tail of occupation number sufficiently with three-momentum cutoff $\Lambda = 0.631$ GeV.

[*) In Ref.14), $G_C/G_S = 0.6$ is adopted where G_C in Ref.14) corresponds to $G_c/2$ here.

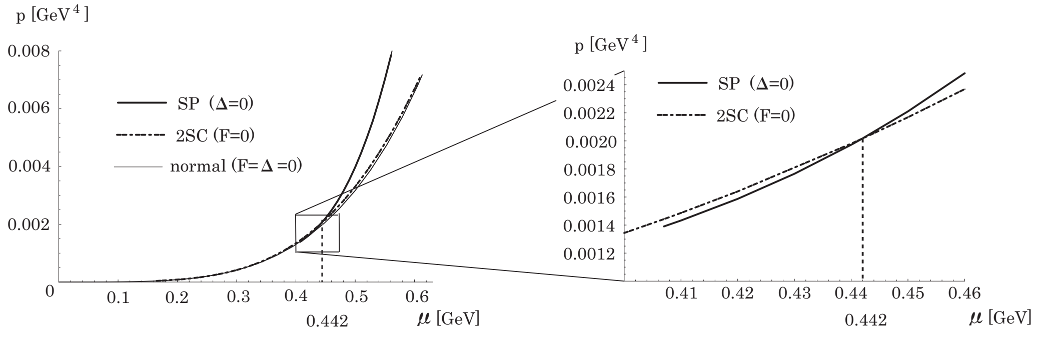

Fig. 1. (a) The pressures for normal (thin curve), two-flavor color superconducting (2SC) (dash-dotted curve) and quark spin polarized (SP) (solid curve) phases are shown as functions with respect to quark chemical potential μ in the case of $\Lambda = 0.631$ GeV . (b) The details are depicted around $\mu \approx 0.442$ GeV.

Since we are interested in the high density region where chiral symmetry is restored, we focus on the transition point from color superconducting phase to the quark spin polarized phase. In Fig. 2, the realized phase is shown by the solid curve. The vertical axis represents the pressure and the horizontal axis represents the baryon number density divided by the normal nuclear density $\rho_0 = 0.17$ fm^{-3} instead of the quark chemical potential by using the relation (4·8). Up to $\rho_B = 4.73\rho_0$, the color superconducting phase is realized. From $\rho_B = 4.73\rho_0$ to $5.84\rho_0$, the color superconducting phase and the quark ferromagnetic phase may coexist. Above $\rho_B = 5.84\rho_0$, the quark spin polarized phase is realized. Thus, the phase transition may be the first order one.

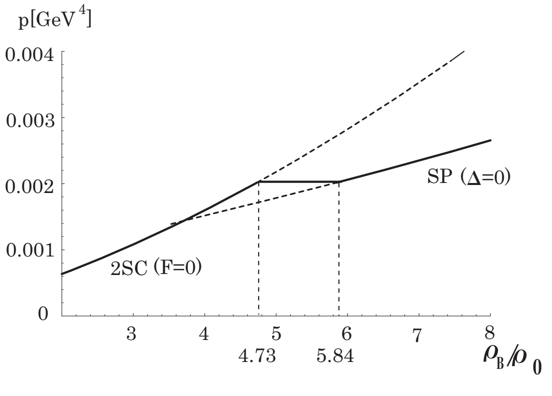

Fig. 2. The realized phase is shown by the solid curve in the case of $\Lambda = 0.631$ GeV. The vertical axis represents the pressure and the horizontal axis represents the baryon number density divided by the normal nuclear density $\rho_0 = 0.17$ fm^{-3}.

§5. Summary and concluding remarks

In this paper, it was shown within the mean field approximation that the quark spin polarized phase is realized succeeding to the two-flavor color superconducting phase as the baryon density increases. We calculated the pressure of the two phases separately, namely, in the 2SC ($\varDelta \neq 0$ and $F = 0$) and the quark spin polarized ($\varDelta = 0$ and $F \neq 0$) phases. As a result, at a certain density region, the 2SC phase is realized. However, at rather high density region, the quark spin polarized phase is realized. If the large F expansion is carried out in Eq.(3·18), then the gap equation for $\varDelta$ is expressed approximately as

$$\varDelta \left[\int \frac{d^3\boldsymbol{p}}{(2\pi)^3} \left(1 + \frac{2\mu\sqrt{p_1^2 + p_2^2} - 3\varDelta^2}{2F^2} \right) - \frac{F}{4G_c} \right] \approx 0 \ . \tag{5·1}$$

For large F, the above equation has only the trivial solution, $\varDelta = 0$. Thus, it is expected actually that the quark spin polarized phase with $\varDelta = 0$ and $F \neq 0$ is realized in the high baryon density region with large F.

For three-momentum cutoff $\varLambda = 0.631$ GeV, the tail of the occupation number is sufficiently taken into account since the value of chemical potential on the phase transition point from 2SC phase to the spin polarized phase is 0.442 GeV. In general in the system with finite chemical potential, a chemical-potential dependent cutoff may be used.$^{17)}$ However, for the sake of comparison, if a rather large fixed value of three-momentum cutoff, $\varLambda = 0.8$ GeV, is adopted where the tail of occupation number is more fully taken into account, the critical chemical potential from 2SC phase to the spin polarized phase is obtained as $\mu = 0.491$ GeV. Above $\mu = 0.491$ GeV, the quark spin polarized phase is realized. With this larger fixed three-momentum cutoff, the following results are obtained: Up to $\rho_B = 7.42\rho_0$, the color superconducting phase is realized. From $\rho_B = 7.42\rho_0$ to $10.86\rho_0$, the color superconducting phase and the quark spin polarized phase may coexist. Above $\rho_B = 10.86\rho_0$, the quark spin polarized phase is realized. The use of large three-momentum cutoff leads to the shift of the phase transition density, that is, the phase transition density is higher with larger three-momentum cutoff.

One of the next task may be to consider the quark-pairing gap $\varDelta$ and the spin polarization F simultaneously. Under this treatment, the behavior of phase transition from 2SC phase with $\varDelta \neq 0$ and $F = 0$ to the quark spin polarized phase with $\varDelta = 0$ and $F \neq 0$ may be clear because the coexistence phase with $\varDelta \neq 0$ and $F \neq 0$ may appear. This is a future problem.

Also, it is important to investigate the interplay between color-flavor locked (CFL) phase and the spin polarized phase at higher density region in quark matter. Further, it may be interesting to investigate the interplay between two quark spin polarized phases, namely, the quark spin polarized phase originated from the tensor-type four-point interaction and that originated from the pseudovector-type four-point interaction between quarks. These topics are left for future problems.

Acknowledgment

One of the authors (Y.T.) would like to express his sincere thanks to Professor J. da Providência and Professor C. Providência, two of co-authors of this paper, for their warm hospitality during his visit to Coimbra in summer of 2012. One of the authors (Y.T.) is partially supported by the Grants-in-Aid of the Scientific Research (No.23540311) from the Ministry of Education, Culture, Sports, Science and Technology in Japan.

References

1) K. Fukushima and T. Hatsuda, Rep. Prog. Phys. **74**, 014001 (2011).
2) T. Kunihiro, T. Muto, T. Takatsuka, R. Tamagaki and T. Tatsumi, Prog. Theor. Phys. Suppl. No.112, 1 (1993).
3) M. Alford, K. Rajagopal and F. Wilczek, Nucl. Phys. B **357**, 443 (1999).
4) K. Iida and G. Baym, Phys. Rev. D **63**, 074018 (2001).
5) M. G. Alford, A. Schmitt, K. Rajagopal and T. Schafer, Rev. Mod. Phys. **80**, 1455 (2008) and references cited therein.
6) L. McLerran and R. D. Pisarski, Nucl. Phys. A **796**, 83 (2007).
7) T. Tatsumi, Phys. Lett. B **489**, 280 (2000).
T. Maruyama and T. Tatsumi, Nucl. Phys. A **693**, 710 (2001).
E. Nakano, T. Maruyama and T. Tatsumi, Phys. Rev. D **68**, 105001 (2003).
8) C. Kouveliotou et al., Nature **393**, 235 (1998).
9) S. Maedan, Prog. Theor. Phys. **118**, 729 (2007).
10) Y. Tsue, J. da Providência, C. Providência and M. Yamamura, Prog. Theor. Phys. **128**, 507 (2012).
11) H. Bohr, P. K. Panda, C. Providência and J. da Providência, arXiv:1203.6272 [nucl-th].
12) H. Bohr, C. Providência and J. da Providência, Eur. Phys. J. A **41**, 355 (2009).
13) Y. Nambu and G. Jona-Lasinio, Phys. Rev. **122**, 345 (1961), Phys. Rev **124**, 246 (1961).
14) M. Kitazawa, T. Koide, T. Kunihiro and Y. Nemoto, Prog. Theor. Phys. **108**, 929 (2002).
15) H. Bohr, P. K. Panda, C. Providência and J. da Providência, Braz. J. Phys. **42**, 68 (2012).
16) T. Hatsuda and T. Kunihiro, Phys. Rep. **247**, 221 (1994).
17) C. H. Lenzi, A. S. Schneider, C. Providência and R. M. Marinho Jr., Phys. Rev. C **82**, 015809 (2010).
R. Casalbuoni, R. Gatto, G. Nardulli and M. Ruggoeri, Phys. Rev. D **68**, 034024 (2003).
M. Baldo, G. F. Burgio, P. Castorina, S. Plumari and Z. Zappal‘a, Phys. Rev. C **75**, 035804 (2007).

Appendix A

—— Mean field Hamiltonian in the basis of good helicity states ——

In the Dirac representation for the Dirac gamma matrices, the Hamiltonian matrix of the spin polarization part, H_{MF}^{SP}, is written as

$$\begin{aligned} h_{MF}^{SP} &= \boldsymbol{p}\cdot\boldsymbol{\alpha} + F\tau_3\beta\Sigma_3 \\ &= \begin{pmatrix} F\tau_3 & 0 & p_3 & p_1 - ip_2 \\ 0 & -F\tau_3 & p_1 + ip_2 & p_3 \\ p_3 & p_1 - ip_2 & -F\tau_3 & 0 \\ p_1 + ip_2 & -p_3 & 0 & F\tau_3 \end{pmatrix} , \end{aligned} \tag{A·1}$$

where $\alpha^i = \gamma^0\gamma^i$ and $\beta = \gamma^0$. For good helicity states, this Hamiltonian matrix is diagonalized with $F = 0$. For simplicity, we rotate around p_3 axis and we set $p_2 = 0$

without loss of generality. In this case, we derive κ in §2 as follows:

$$\begin{aligned}
U &= \frac{1}{2\sqrt{p}}\left(\begin{array}{cccc}
\sqrt{p+p_3} & \sqrt{p-p_3} & -\sqrt{p+p_3} & -\sqrt{p-p_3} \\
\frac{p_1}{|p_1|}\sqrt{p-p_3} & -\frac{p_1}{|p_1|}\sqrt{p+p_3} & -\frac{p_1}{|p_1|}\sqrt{p-p_3} & \frac{p_1}{|p_1|}\sqrt{p+p_3} \\
\sqrt{p+p_3} & -\sqrt{p-p_3} & \sqrt{p+p_3} & -\sqrt{p-p_3} \\
\frac{p_1}{|p_1|}\sqrt{p-p_3} & \frac{p_1}{|p_1|}\sqrt{p+p_3} & \frac{p_1}{|p_1|}\sqrt{p-p_3} & \frac{p_1}{|p_1|}\sqrt{p+p_3}
\end{array}\right) , \\
\kappa &= U^{-1}h_{MF}^{SP}U \\
&= \left(\begin{array}{cccc}
p & 0 & 0 & 0 \\
0 & p & 0 & 0 \\
0 & 0 & -p & 0 \\
0 & 0 & 0 & -p
\end{array}\right) + \frac{F\tau_3}{p}\left(\begin{array}{cccc}
0 & |p_1| & -p_3 & 0 \\
|p_1| & 0 & 0 & p_3 \\
-p_3 & 0 & 0 & |p_1| \\
0 & p_3 & |p_1| & 0
\end{array}\right) . \qquad (A\cdot 2)
\end{aligned}$$

Finally, in the original basis rotated around p_3-axis, $|p_1|$ is replaced to $\sqrt{p_1^2+p_2^2}$ and we get the result given in Eq. (2·5) in §2.